NaF/KF Post-Deposition Treatments and their Influence on the Structure of Cu(In,Ga)Se_2 Absorber Surfaces

Evelyn Handick,[1] Patrick Reinhard,[2] Regan G. Wilks,[1,3] Fabian Pianezzi,[2] Roberto Félix,[1] Mihaela Gorgoi,[1] Thomas Kunze,[1] Stephan Buecheler,[2] Ayodhya N. Tiwari,[2] and Marcus Bär[1,3,4]

[1]Helmholtz-Zentrum Berlin für Materialien und Energie GmbH, Hahn-Meitner Platz 1, 14109 Berlin, Germany
[2]Laboratory of Thin Films and Photovoltaics, Empa-Swiss Federal Laboratories for Materials and Science and Technology, Überlandstraße 129, 8600 Dübendorf, Switzerland
[3]Energy Materials In-Situ Laboratory Berlin (EMIL), Helmholtz-Zentrum Berlin für Materialien und Energie GmbH, Albert-Einstein-Straße 15, 12489 Berlin, Germany
[4]Institut für Physik und Chemie, Brandenburgische Technische Universität Cottbus-Senftenberg, Platz der Deutschen Einheit 1, 03046 Cottbus, Germany

***Abstract* — To determine the influence of NaF/KF-post-deposition treatments (PDT) on the chemical and topographical surface structure of Cu(In,Ga)Se_2 (CIGSe) solar cell absorbers, we have used synchrotron-based hard x-ray photoelectron spectroscopy (HAXPES) and scanning electron microscopy (SEM). Variations of the PDT parameters can be used to tune thickness and degree of surface nanopatterning; here we find that the nanopatterning is more pronounced on CIGSe surfaces having more potassium and less copper and gallium. Detailed analysis of Se 3d and In 4d photoemission spectra reveals the presence of (at least) two different species, which indicate the formation of a (nanopatterned) K-In-Se-type surface layer.**

***Index Terms* — alkali post-deposition treatment, chalcopyrite thin-film solar cells, chemical structure, hard x-ray photoelectron spectroscopy.**

I. Introduction

The latest boost in Cu(In,Ga)Se_2 (CIGSe)-based solar cell efficiencies lead to devices with a performance of over 22%.[1] Such an achievement shows the high potential of this thin-film photovoltaic (PV) technology as a viable alternative to polycrystalline silicon-wafer based solar cell devices – the currently dominating PV technology. The recent gain in CIGSe cell efficiencies is ascribed to the addition of alkalis into the CIGSe material. Sodium – incorporated into the absorber by (uncontrolled) diffusion from the underlying soda lime glass substrate – is known to modify the CIGSe properties and improve the cell efficiency.[2]–[5] A controlled incorporation of alkali elements in the absorber by means of a post-deposition treatment (PDT) employing alkali-fluorides helps to further enhance performance.[6]–[8] While it was shown that a combined NaF/KF-PDT significantly enhances the device efficiency [7], its impact on the chemical, electronic, and topographical absorber structure is poorly understood.

It has been reported that the NaF/KF-PDT can result in a "nanopatterned" surface topography [9] and produces a copper- and gallium-depleted and potassium-containing surface region.[7], [10], [11] Furthermore, it was shown that this treatment has a distinct effect on the electronic surface structure of CIGSe absorbers.[8], [10] We have previously found a pronounced surface band gap (E_g^{surf}) widening – explained by the formation of the Cu- and Ga-depleted surface and a K-In-Se type surface species – resulting in E_g^{surf}=(2.52[+0.14/-0.51] eV).[10]

In order to properly evaluate the impact of these CIGSe surface modifications on the performance of resulting solar cells, the degree of surface nanopatterning [9], i.e., the presence and thickness of a possible noncontinuous surface layer with different optoelectronic properties on top of the absorber, must be considered. The extent of nanopatterning – and here in particular the domain size and surface region thickness − should be taken into account when discussing the effect of the surface layer on device efficiency. As pointed out in Ref. [10], in the case of a sufficient thickness of the surface region (to act as a passivation layer) with very distinct nanopatterning (i.e., similar geometrical features as in Ref. [9]) the presence of point openings in the surface layer is possible. Based on simulations, [9] such "point contacts" could partly explain the beneficial effect of the NaF/KF-PDT treatment on the open circuit voltage and fill factor of corresponding CIGSe-based devices. In the case of a thin surface region and/or only loosely distributed domains (i.e., the nanopatterning is [almost] nonexistent as reported in Ref. [12]), then the downward shift of the VBM could explain the improved performance by an increased charge selectivity more efficiently repelling holes from the emitter/absorber contact. Such a downward shift is reported to be more pronounced for NaF/KF-PDT CIGSe (compared to NaF-PDT CIGSe) [10]. However, these arguments assume that the chemical and electronic properties of the surface layer are not directly influenced by the PDT parameters in the same way as is the formation and extent of the nanopatterned surface layer.

In order to study how the surface structure of NaF/KF-PDT CIGSe samples depends on the PDT

parameters, we combine non-destructive synchrotron-based hard x-ray photoelectron spectroscopy (HAXPES) together with scanning electron microscopy (SEM) analysis. While HAXPES was employed to reveal and compare the chemical structure of an *alkali-free* (i.e. untreated) CIGSe absorber with two differently treated NaF/KF-PDT CIGSe absorbers, SEM was used to gain information about the surface topography (i.e., the degree of surface nanopatterning).

II. Experimental

A low-temperature multistage process was used to deposit CIGSe onto molybdenum-coated polyimide foil. [7] Subsequently, two types of NaF/KF-post-deposition treatment of the as-prepared CIGSe absorbers were carried out according to Ref. [7]. A PDT comprises of depositing thin films of alkali fluorides (NaF and KF) on top of the CIGSe absorber at elevated temperature in Se atmosphere. The main difference between the PDTs compared in this study is the evaporation rate of the alkali fluorides. Rates of approximately 1.5-2 and 1-1.5 nm/min were used for the different NaF/KF-PDTs, resulting in an *alkali-rich* and an *alkali-poor* CIGSe sample. Influence of other process fluctuations such as Se overpressure during PDT or a slightly different CIGS surface composition can also not be excluded. To minimize surface contamination, all samples were packed and sealed in a N_2-filled glovebag attached to the deposition chamber at Empa immediately after sample preparation. After transport of the sealed samples to the HZB, the samples were re-sealed in a N_2-filled glovebox for storage. The remaining NaF/KF capping layer was removed before analysis by immersing the samples in aqueous ammonia solution (0.1 mol/l) for 1-2 min followed by a rinsing step with deionized (DI) H_2O before vacuum-drying. No additional cleaning of the sample surface was performed before measurements. After characterizing the samples with HAXPES, they were sent back to Empa in nitrogen atmosphere for topography analysis by SEM.

Scanning electron microscopy (SEM) was performed at Empa using a Hitachi S-4800 with an in-lens detector. An acceleration voltage of 5 kV, a working distance of 5 mm and a magnification of 60,000 were used for the measurements.

Synchrotron-based hard x-ray photoelectron spectroscopy (HAXPES) experiments were conducted at the HiKE endstation [13] on the KMC-1 beamline [14] of the BESSY-II electron storage ring. The samples were introduced into the system with a short air exposure (< 2 min). The endstation is equipped with a Scienta R4000 electron energy analyzer and its base pressure was $<1\times10^{-8}$ mbar during analysis. The beamline is equipped with a double crystal monochromator (DCM) that allows tuning the excitation energy between 2.0 and 10.0 keV. Spectra were recorded using photon energies of about 2 keV employing the Si(111) DCM crystals. A pass energy of 500 eV was used for measuring the survey spectra and 200 eV for the detail spectra of the shallow core levels (K 2p, Cu 3p, Se 3d, K 3s, In 4d, Ga 3d, and K 3p). Energy calibration was done by measuring the Au 4f detail spectrum of a clean gold foil and setting the Au $4f_{7/2}$ binding energy to 84.00 eV. For detail spectra the combined analyzer plus beamline resolution is approximately 0.25 eV.

III. Results and Discussion

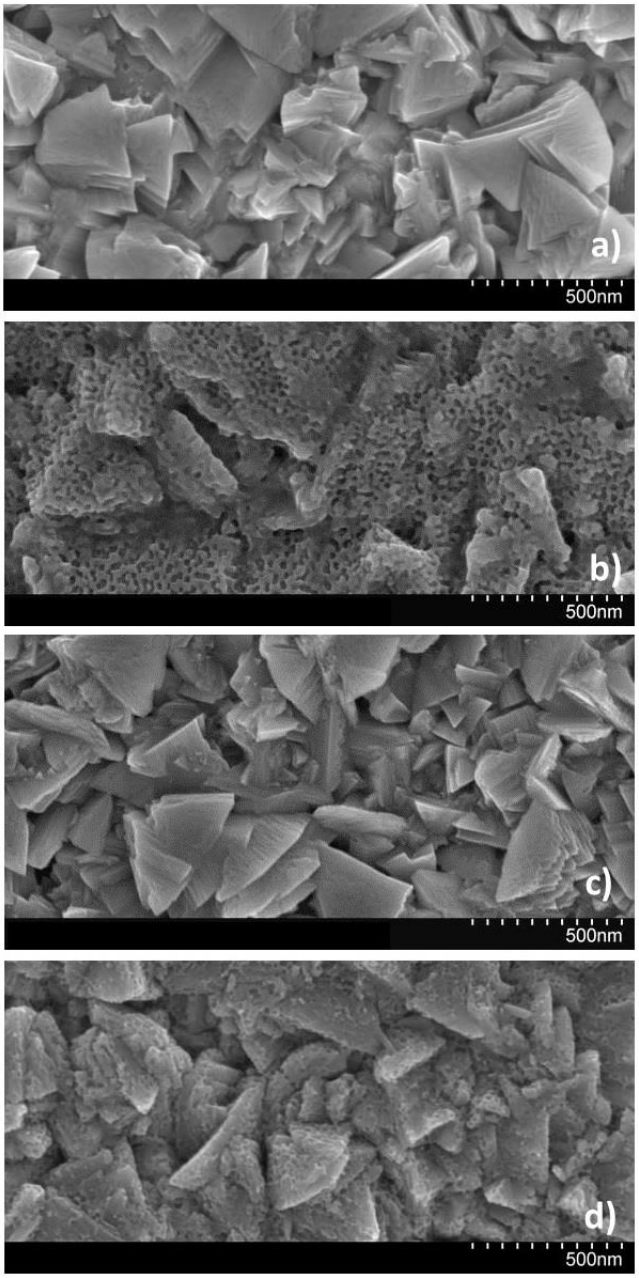

Fig. 1. SEM images of differently treated $Cu(In,Ga)Se_2$ (CIGSe) absorbers. Images a) and c) show the topography of the *alkali-free* absorbers and image b) and d) show the respective NaF/KF-PDT CIGSe samples that got an *alkali-rich* b) and an *alkali-poor* PDT d), respectively.

Fig. 1 shows the SEM top-view images of the *alkali-free* and NaF/KF-PDT CIGSe samples. From Fig. 1 b) and d), one can confirm the formation of a nanopatterned surface structure in agreement with Ref. [9]. The structure becomes very apparent when comparing to the SEM images of the respective *alkali-free* absorbers that are shown in Fig. 1a) and c), respectively. While the nanopatterned surface layer almost completely covers the facet-like CIGSe topography for the *alkali-rich* NaF/KF-PDT CIGSe (Fig. 1b), for the *alkali-poor* NaF/KF-PDT CIGSe sample (Fig. 1d) we find that the facet-like topography of the underlying CIGSe absorber can still be recognized. From this we can conclude that a thicker surface layer with more distinct nanopatterning features is formed on the *alkali-rich* than on the *alkali-poor* NaF/KF-PDT CIGSe sample.

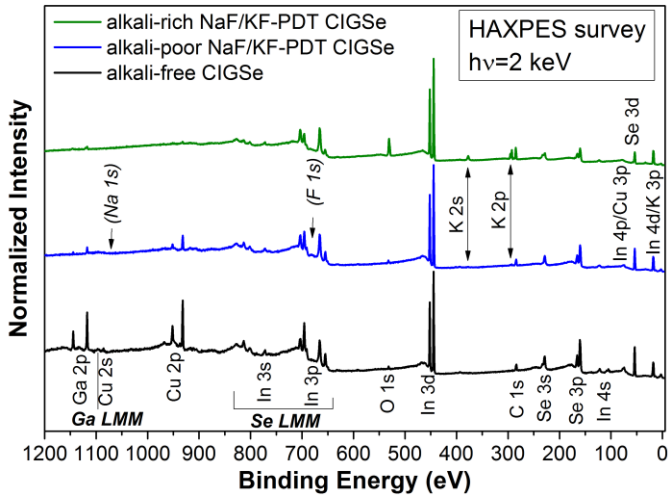

Fig. 2. HAXPES survey spectra (normalized to In 3d height) of differently treated Cu(In,Ga)Se_2 (CIGSe) absorbers taken with an excitation energy of hν = 2 keV. The spectrum of the *alkali-free* CIGSe (black) is compared to the spectra of absorbers that underwent an *alkali-poor* NaF/KF (blue) post-deposition treatment (PDT) and an *alkali-rich* NaF/KF-PDT (green), respectively.

To determine if there is a correlation between the extent of nanopatterned surface layer and the chemical structure of the CIGSe surface, HAXPES measurements were performed. From the survey spectra measured with an excitation energy of hν = 2 keV – resulting in an inelastic mean free path (IMFP) of the detected photoelectrons of at most 4 nm [15] – shown in Fig. 2, it can be seen that the surface of both NaF/KF-PDT absorbers is gallium- and copper-depleted and contains potassium (but no fluorine or sodium) as previously reported.[7], [10]

In contrast, for the *alkali-free* CIGSe absorber all expected CIGSe-related photoemission lines are present, with intensity in accordance with a Cu-poor Cu:(In+Ga):Se composition, in agreement with previous reports.[16], [17] Note that the *alkali-free* CIGSe spectra shown in Fig. 2 and 3 belong to the sample shown in Fig. 1c) and prepared in the same absorber deposition run as the *alkali-poor* CIGSe absorber; the spectra of the *alkali-free* CIGSe (Fig. 1a) related to the *alkali-rich* CIGSe are very similar. For the NaF/KF-PDT CIGSe samples, we detect no Na signal, which may be due to the suggested "ion-exchange mechanism" explaining that K replaces Na in the CIGSe during the PDT.[7], [18] Comparing the two NaF/KF-PDT CIGSe absorbers, it is apparent that for the *alkali-poor* NaF/KF-PDT CIGSe the intensity of the K-related photoemission signals (K 2s and K 2p) is significantly lower than the respective peak intensities for the *alkali-rich* NaF/KF-PDT CIGSe (see also Fig. 3c2)). At the same time, the degree of Cu- and Ga-depletion is less pronounced. Note that for all CIGSe absorbers, significant oxygen and carbon signals are detected. These elements are likely due to surface contamination; however, the trend of increasing O 1s intensity with increasing potassium surface content may also indicate alkali-promoted CIGSe surface oxidation.

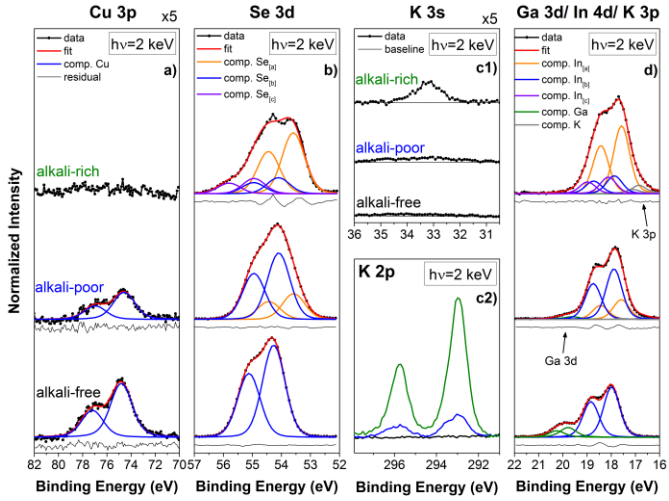

Fig. 3. HAXPES (shallow) core level spectra of an *alkali-free* CIGSe absorber (bottom spectra) and of an *alkali-poor* (center spectra) / *alkali-rich* (top spectra) NaF/KF-PDT CIGSe sample: Cu 3p (a), Se 3d (b), K 3s (c1), K 2p (c2), and Ga 3d/In 4d/K 3p (d). The respective fits using Voigt profiles (doublets) including the resulting residuals (difference between data and fit) are also shown. For the Se 3d and In 4d spectra of the NaF/KF PDT CIGSe samples more than one component ("comp.") is required to obtain a reasonable fit. All spectra (except K 2p) are area-normalized to the Se 3d peak area and shown with the respective linear background subtracted. For better visibility the Cu 3p and K 3s spectra are depicted magnified by a factor of ×5. The K 2p spectra are normalized to the background.

To gain a more detailed picture of the chemical structure differences – without having to consider different IMFPs and electron analyzer transmission – the shallow core levels Cu 3p, Se 3d, K 3s, and Ga 3d/In 4d/K 3p of the extended valence band are analyzed. Fig. 3 shows the results of the curve fit analysis of the measured shallow core levels, simultaneously fitted by using Voigt profiles with linked width and shape for each core level line. A linear background was included in the

fit procedure but is subtracted from the spectra shown in Fig. 3. For the Cu 3p line (Fig. 3a) the doublet separation was set to 2.39 eV [15] and the underlying In 4p background (derived from measurement of a Cu-free K-In-Se type reference sample) was subtracted before the fit (for more details see Ref. [11]). As discussed above, the Cu depletion is significantly more pronounced for the *alkali-rich* compared to the *alkali-poor* NaF/KF-PDT (and *alkali-free*) CIGSe. For the fit of the Se 3d doublet (Fig. 3b) a separation of 0.83 eV was used.[19] For both NaF/KF-PDT CIGSe samples two/three components are needed to properly represent the Se 3d spectrum while that of the *alkali-free* CIGSe can be fitted with one spin-orbit doublet. The orange doublet ($Se_{[a]}$) is ascribed to a K-In-Se type surface species as suggested in Refs. [10], [11]. Consequently, the blue doublet ($Se_{[b]}$) is attributed to the (underlying/not covered) CIGSe absorber. The additional purple doublet ($Se_{[c]}$) that can be observed for the *alkali-rich* NaF/KF-PDT CIGSe can most likely be attributed to an In-Se-O compound [20] presumably formed due to a (alkali-promoted) surface oxidation. Panel 3c1) displays the region of the K 3s photoemission line. In agreement with the survey spectra related discussion above, it can again be clearly observed that the potassium surface content is higher for the *alkali-rich* compared to the *alkali-poor* NaF/KF-PDT CIGSe sample. This is more clearly shown by the K 2p core level spectra, displayed in Fig. 3c2), which has a 3 times higher photoionization cross-section than K 3s [21]. The broader K 2p and K 3s peak of the *alkali-poor* sample (blue spectrum in Fig. 3c2 and center spectrum in c1) may indicate the presence of more than one potassium species. Fig. 3d) shows the energy range of the Ga 3d/ In 4d/ K 3p photoemission lines. The doublet separations used for the fits were: 0.46 eV for Ga 3d,[22] 0.86 eV for In 4d,[23] and 0.25 eV for K 3p [24]. As with Se 3d two/three components are required to fit the In 4d line properly. Component $In_{[a]}$ is again ascribed to a K-In-Se type surface species [10], $In_{[b]}$ is assigned to the (underlying/not covered) CIGSe absorber, and $In_{[c]}$ represents the In-Se-O like compound [20] exclusively formed on the *alkali-rich* NaF/KF-PDT CIGSe absorber. Note that for the very complex fit of the Ga 3d/ In 4d/ K 3p region the $In_{[a]}/In_{[b]}$ ratio was set equal to the $Se_{[a]}/Se_{[b]}$ ratio; i.e., the assumption that the same species are observed in the In and Se photoemission is "built in" to the fit. Additionally, as another constraint the K 3p line is linked to K 3s in area and position using the respective photoionization cross-sections [21] and the difference in binding energy of K 3s (34.70 eV [25]) and K $3p_{3/2}$ (18.34 eV [24]) line of 16.36 eV. No Ga 3d contribution is required to get to a reasonable fit of this spectral range for the *alkali-rich* NaF/KF PDT CIGSe, in agreement with the discussion above.

The Cu and Ga levels of the *alkali-rich* NaF/KF-PDT CIGSe absorber surface are below the HAXPES detection limit. In comparison, the *alkali-poor* NaF/KF-PDT CIGSe sample has a significantly higher surface content of Cu and Ga but exhibits lower Cu and Ga amounts than the *alkali-free* absorber. The surface potassium varies: it is highest for the *alkali-rich* NaF/KF-PDT-CIGSe, detectable (but significantly lower) for the *alkali-poor* NaF/KF-PDT CIGSe, and (as expected) not detectable for the *alkali-free* absorber. Component [a] of the Se and In photoemission lines found at lower binding energies and ascribed to a K-In-Se type surface compound is clearly more pronounced for the *alkali-rich* treated NaF/KF-PDT CIGSe than for the *alkali-poor* counterpart. Conversely, the spectra of the *alkali-poor* NaF/KF-PDT CIGSe show a larger CIGSe related component ($\rightarrow$ [b]). Component [b] is located at higher binding energies which are in agreement with the respective photoemission lines of the *alkali-free* absorber, confirming this attribution.

Based on these findings, we suggest that a K-In-Se/CIGSe bilayer system is formed in which the (nanopatterned) K-In-Se thickness/coverage can be "tuned" via the NaF/KF-PDT parameters.

IV. Conclusion

By using SEM and HAXPES, we studied the impact of different NaF/KF-PDT parameters (and here in particular the thickness of the NaF/KF bilayer) on the surface structure of CIGSe thin-film solar cell absorbers. With increasing amounts of alkali fluorides, we find a more pronounced degree of nanopatterning combined with a higher degree of Cu- and Ga-depletion and K-content at the absorber surface. Combined analysis of the SEM and HAXPES data suggests the formation of a (nanopatterned) K-In-Se – type surface layer on top of the underlying CIGSe that can be tuned in thickness by the PDT parameters. Furthermore, we find indications for an (alkali-promoted) CIGSe surface oxidation for high amounts of potassium. These NaF/KF-PDT induced changes in surface structure of the chalcopyrite thin-film solar cell absorber could also impact the CdS deposition and therefore might influence the properties of the buffer/CIGSe interface.

Acknowledgement

E. Handick, R.G. Wilks, R. Félix, T. Kunze, and M. Bär acknowledge the Helmholtz-Association (VH-NG-423) for financial support. Furthermore, this work has received funding from the European Union's Horizon 2020 research and innovation Programme under grant agreement No 641004 (Sharc25) and has been supported by the Swiss State Secretariat for Education, Research and Innovation (SERI) under contract number REF-1131-52107.

References

[1] "Solar Frontier Achieves World Record Thin-Film Solar Cell Efficiency: 22.3%." [Online]. Available: http://www.solar-frontier.eu/en/aktuelles/press-releases/2015/detail/?tx_ttnews[tt_news]=1179&cHash=39a1d48f83f991dc116d30b3224caea0. [Accessed: 15-Dec-2015].

[2] M. B. Zellner, R. W. Birkmire, E. Eser, W. N. Shafarman, and J. G. Chen, "Determination of activation barriers for the diffusion of sodium through CIGS thin-film solar cells," *Prog. Photovolt. Res. Appl.*, vol. 11, no. 8, pp. 543–548, Dec. 2003.

[3] A. Rockett, K. Granath, S. Asher, M. M. Al Jassim, F. Hasoon, R. Matson, B. Basol, V. Kapur, J. S. Britt, T. Gillespie, and C. Marshall, "Na incorporation in Mo and $CuInSe_2$ from production processes," *Sol. Energy Mater. Sol. Cells*, vol. 59, no. 3, pp. 255–264, Oct. 1999.

[4] C. Heske, R. Fink, E. Umbach, W. Riedl, and F. Karg, "Na-induced effects on the electronic structure and composition of $Cu(In,Ga)Se_2$ thin-film surfaces," *Appl. Phys. Lett.*, vol. 68, no. 24, pp. 3431–3433, Jun. 1996.

[5] X. Song, R. Caballero, R. Félix, D. Gerlach, C. A. Kaufmann, H.-W. Schock, R. G. Wilks, and M. Bär, "Na incorporation into $Cu(In,Ga)Se_2$ thin-film solar cell absorbers deposited on polyimide: Impact on the chemical and electronic surface structure," *J. Appl. Phys.*, vol. 111, no. 3, p. 34903, Feb. 2012.

[6] P. Jackson, D. Hariskos, R. Wuerz, O. Kiowski, A. Bauer, T. M. Friedlmeier, and M. Powalla, "Properties of $Cu(In,Ga)Se_2$ solar cells with new record efficiencies up to 21.7%," *Phys. Status Solidi RRL – Rapid Res. Lett.*, vol. 9, no. 1, pp. 28–31, Jan. 2015.

[7] A. Chirilă, P. Reinhard, F. Pianezzi, P. Bloesch, A. R. Uhl, C. Fella, L. Kranz, D. Keller, C. Gretener, H. Hagendorfer, D. Jaeger, R. Erni, S. Nishiwaki, S. Buecheler, and A. N. Tiwari, "Potassium-induced surface modification of $Cu(In,Ga)Se_2$ thin films for high-efficiency solar cells," *Nat. Mater.*, vol. 12, no. 12, pp. 1107–1111, Dec. 2013.

[8] P. Pistor, D. Greiner, C. A. Kaufmann, S. Brunken, M. Gorgoi, A. Steigert, W. Calvet, I. Lauermann, R. Klenk, T. Unold, and M.-C. Lux-Steiner, "Experimental indication for band gap widening of chalcopyrite solar cell absorbers after potassium fluoride treatment," *Appl. Phys. Lett.*, vol. 105, no. 6, p. 63901, Aug. 2014.

[9] P. Reinhard, B. Bissig, F. Pianezzi, H. Hagendorfer, G. Sozzi, R. Menozzi, C. Gretener, S. Nishiwaki, S. Buecheler, and A. N. Tiwari, "Alkali-Templated Surface Nanopatterning of Chalcogenide Thin Films: A Novel Approach Toward Solar Cells with Enhanced Efficiency," *Nano Lett.*, vol. 15, no. 5, pp. 3334–3340, May 2015.

[10] E. Handick, P. Reinhard, J.-H. Alsmeier, L. Köhler, F. Pianezzi, S. Krause, M. Gorgoi, E. Ikenaga, N. Koch, R. G. Wilks, S. Buecheler, A. N. Tiwari, and M. Bär, "Potassium Postdeposition Treatment-Induced Band Gap Widening at $Cu(In,Ga)Se_2$ Surfaces – Reason for Performance Leap?," *ACS Appl. Mater. Interfaces*, vol. 7, no. 49, pp. 27414–27420, Dec. 2015.

[11] E. Handick, P. Reinhard, R. G. Wilks, F. Pianezzi, D. Kreikemeyer-Lorenzo, L. Weinhardt, M. Blum, W. Yang, M. Gorgoi, E. Ikenaga, D. Gerlach, S. Ueda, Y. Amashita, T. Chikyow, C. Heske, S. Buecheler, A. N. Tiwari, and M. Bär, "NaF/KF post-deposition treatment induced formation of a K-In-Se – type surface species on $Cu(In,Ga)Se_2$ thin-film solar cell absorbers," *in progress*, 2016.

[12] P. Jackson, D. Hariskos, R. Wuerz, O. Kiowski, A. Bauer, and M. Powalla, "Properties of High Efficiency $Cu(In,Ga)Se_2$ Solar Cells," presented at the 2015 MRS Spring Meeting & Exhibit; B7.02, San Francisco, 09-Apr-2015.

[13] M. Gorgoi, S. Svensson, F. Schäfers, G. Öhrwall, M. Mertin, P. Bressler, O. Karis, H. Siegbahn, A. Sandell, H. Rensmo, W. Doherty, C. Jung, W. Braun, and W. Eberhardt, "The high kinetic energy photoelectron spectroscopy facility at BESSY progress and first results," *Nucl. Instrum. Methods Phys. Res. Sect. Accel. Spectrometers Detect. Assoc. Equip.*, vol. 601, no. 1–2, pp. 48–53, Mar. 2009.

[14] F. Schaefers, M. Mertin, and M. Gorgoi, "KMC-1: A high resolution and high flux soft x-ray beamline at BESSY," *Rev. Sci. Instrum.*, vol. 78, no. 12, p. 123102, Dec. 2007.

[15] S. Tanuma, C. J. Powell, and D. R. Penn, "Calculations of electron inelastic mean free paths. V. Data for 14 organic compounds over the 50–2000 eV range," *Surf. Interface Anal.*, vol. 21, no. 3, pp. 165–176, Mar. 1994.

[16] M. Morkel, L. Weinhardt, B. Lohmüller, C. Heske, E. Umbach, W. Riedl, S. Zweigart, and F. Karg, "Flat conduction-band alignment at the $CdS/CuInSe_2$ thin-film solar-cell heterojunction," *Appl. Phys. Lett.*, vol. 79, no. 27, pp. 4482–4484, Dec. 2001.

[17] M. Bär, S. Nishiwaki, L. Weinhardt, S. Pookpanratana, O. Fuchs, M. Blum, W. Yang, J. D. Denlinger, W. N. Shafarman, and C. Heske, "Depth-resolved band gap in $Cu(In,Ga)(S,Se)_2$ thin films," *Appl. Phys. Lett.*, vol. 93, no. 24, p. 244103, Dec. 2008.

[18] P. Reinhard, B. Bissig, F. Pianezzi, E. Avancini, H. Hagendorfer, D. Keller, P. Fuchs, M. Döbeli, C. Vigo, P. Crivelli, S. Nishiwaki, S. Buecheler, and A. N. Tiwari, "Features of KF and NaF Postdeposition Treatments of $Cu(In,Ga)Se_2$ Absorbers for High Efficiency Thin Film Solar Cells," *Chem. Mater.*, vol. 27, no. 16, pp. 5755–5764, Aug. 2015.

[19] N. J. Shevchik, M. Cardona, and J. Tejeda, "X-Ray and Far-uv Photoemission from Amorphous and Crystalline Films of Se and Te," *Phys. Rev. B*, vol. 8, no. 6, pp. 2833–2841, Sep. 1973.

[20] A. J. Nelson, S. Gebhard, L. L. Kazmerski, E. Colavita, M. Engelhardt, and H. Höchst, "Characterization of the native oxide of $CuInSe_2$ using synchrotron radiation photoemission," *Appl. Phys. Lett.*, vol. 57, no. 14, pp. 1428–1430, Oct. 1990.

[21] M. B. Trzhaskovskaya, V. I. Nefedov, and V. G. Yarzhemsky, "Photoelectron Angular Distribution Parameters for Elements Z=1 to Z=54 in the Photoelectron Energy Range 100-5000 eV," *At. Data Nucl. Data Tables*, vol. 77, no. 1, pp. 97–159, Jan. 2001.

[22] D. M. Poirier and J. H. Weaver, "GaAs(110) by XPS," *Surf. Sci. Spectra*, vol. 2, no. 3, pp. 201–208, Jul. 1993.

[23] R. T. Poole, P. C. Kemeny, J. Liesegang, J. G. Jenkin, and R. C. G. Leckey, "High resolution photoelectron studies of the d bands of some metals," *J. Phys. F Met. Phys.*, vol. 3, no. 3, p. L46, 1973.

[24] G. K. Wertheim and D. M. Riffe, "Evidence for crystal-field splitting in surface-atom photoemission from potassium," *Phys. Rev. B*, vol. 52, no. 20, pp. 14906–14910, Nov. 1995.

[25] L.-G. Petersson and S.-E. Karlsson, "Clean and Oxygen Exposed Potassium Studied by Photoelectron Spectroscopy," *Phys. Scr.*, vol. 16, no. 5–6, pp. 425–431, Nov. 1977.